Physical modelling of static liquefaction of seabed

Modélisation physique de la liquéfaction statique des fonds marins

Amin Askarinejad

Department of Geo-Sciences and Engineering, TU Delft, Delft, The Netherlands

Weiyuan Zhang

Department of Geo-Sciences and Engineering, TU Delft, Delft, The Netherlands

Arash Maghsoudloo

Department of Geo-Sciences and Engineering, TU Delft, Delft, The Netherlands

ABSTRACT: Sudden instabilities around hydraulic structures can be triggered due to the gradual increase of seabed inclination as result of souring process. This article compares the results of physical modelling of two corresponding submarine landslides induced by static liquefaction. One of the landslides has been triggered using a 1g large-scale Liquefaction Tank and serves as the prototype for the second landslide which was triggered using a newly developed static liquefaction actuator in a geotechnical centrifuge at 10g. The details of the centrifuge test setup designed to simulate the statically liquefied small-scale landslide are discussed and compared to the 1g test.

RÉSUMÉ: Des instabilités soudaines autour des structures hydrauliques peuvent être provoquées par l'augmentation progressive de l'inclinaison des fonds sous-marins résultant du processus de acidification. Cet article compare les résultats de la modélisation physique de deux glissements de terrain sous-marins correspondants. L'un des glissements de terrain a été déclenché à l'aide d'un réservoir de liquéfaction à grande échelle à 1 g et sert de prototype pour le deuxième glissement de terrain qui a été déclenché à l'aide d'un actionneur de liquéfaction statique récemment développé dans une centrifugeuse géotechnique à 10 g. Les détails de la configuration de test de centrifugation conçue pour simuler les glissements de terrain à petite échelle liquéfiés statiquement sont discutés et comparés aux tests de 1g.

Keywords: Static Liquefaction, Submarine landslides, Physical Modelling, Geotechnical Centrifuge

1 INTRODUCTION

Several case histories have been reported in the literature on the failure of submerged loose sandy slopes which had been generated by the erosion processes of waves and currents around hydraulic structures. One example of this type of flow slides happened in the vicinity of the Easter Scheldt storm Surge barrier in the South Western part of the Netherlands. However, lack of information on the triggers due to abruptness of the phenomenon and difficulty in monitoring makes it challenging to develop prediction models. This type of instability, often called static liquefaction, occurs in saturated loose sand layers due to sudden reduction of effective stresses to zero caused by generation of excess pore pressure under a minor monotonic change in the shearing load (Sladen et al. 1985; Kramer 1988; Lade 1992;

Take et al. 2004; Masson et al. 2006; De Groot et al. 2012).

Most of the experimental studies of this behaviour of sandy soils are limited to triaxial compression tests under undrained conditions (e.g, Chu et al. 2003) which applies a simplified loading scenario to the samples. However, the real stress path that a soil element in a submerged slope experiences up to failure is still not fully understood, and this makes the results of the element tests limited to the applied predefined stress paths in the triaxial tests. Therefore, application of physical modelling in understanding the process leading to the flow slides is considered as a useful approach. Nonetheless, there are limited number of studies of the static liquefaction failures using physical modelling (Eckersley 1990; Byrne et al. 2000; Askarinejad et al. 2018). De Jager et al. (2017) designed a 1g large scale Liquefaction Tank at TU Delft with the main purpose of investigating slope over-steepening effect on inducing under-water liquefaction. However, the maximum height of the soil layer in this facility is 1.5 m. Therefore, a novel actuator has been developed at section of Geo-Engineering of TU Delft to study this phenomenon for larger slopes.

This paper discusses the results of two tests aiming at physical modelling of static liquefaction in submerged slopes using the large-scale Liquefaction Tank and small-scale centrifuge models.

2 SCALING LAW FOR STATIC LIQUEFACTION

The internal mechanism leading to static liquefaction can be explained by the collapse of saturated voids, which results in local and abrupt increase of the pore pressure (Askarinejad et al. 2014). The locally increased pore pressure reduces the effective stress and hence the shear strength, and can trigger movements in the soil mass. Therefore, the main focus is on the grain scale and structure of the soil used in modelling

the static liquefaction process as illustrated in **Error! Reference source not found.**. The scaling factor of the length (L) in the grain scale will be $L_p/L_m=1$ (the subscripts p and m stand for prototype and model, respectively)**.**

The time scale for gravitational falling (T_{impact}) of a particle at grain scale would be:

$$T_{impact} = \sqrt{\frac{2L}{a}}, \qquad \frac{L_m}{L_p} = 1,$$

$$\frac{a_m}{a_p} = N \implies \frac{T_{impact,m}}{T_{impact,p}} \qquad (1)$$

$$= \sqrt{\frac{1}{N}}$$

where L is the falling height, and a is the acceleration.

Falling of a particle on a water saturated void results in sudden increase in the pore fluid pressure. The rate of dissipation of this excess pore pressure can be calculated using Darcy's law (Darcy 1856).
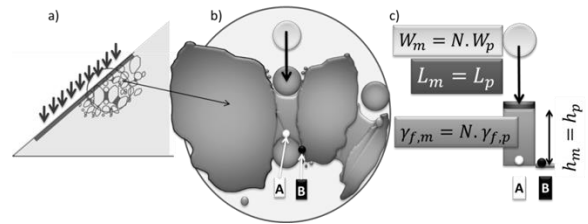

Figure 1. Schematic of the collapse of voids leading to local generation of excess pore pressures. a) at real scale, b) zoomed in grain scale, and c) simplified small scale model in the centrifuge, W is the weight of a grain and γ_f is the unit weight of the pore fluid (After Askarinejad et al. 2014).

It can be concluded that under Ng acceleration, the impact time of a particle is reduced by a factor of $\sqrt{1/N}$, while the localised dissipation of the excess pore fluid pressure will be N times faster

than the prototype (Askarinejad et al. 2014). This means that the increased acceleration provides a condition in which the excess pore pressure dissipates $\sqrt{N}$ faster than the collapse of the soil structure. Therefore, a pore fluid $\sqrt{N}$-times more viscous than water is used in the centrifuge test of this study to reduce the dissipation time in the model.

3 MATERIAL CHARACTERIZATION

A very fine, uniform silica sand is used for both experiments of this study. Table 1 summarizes the geotechnical properties of the sand.

Table 1. Geotechnical properties of the soil)

Parameter	Values
D_{50} (mm)	0.11
$\varphi'_{residual}$ (Deg)	36
Permeability (m/s)	4.2E-5
Min-Max void ratio (-)	0.64-1.07
Particle shape	Sub-rounded

Figure 2 illustrates the grain size distribution of the nine samples that were collected from nine different locations of the sand batch.
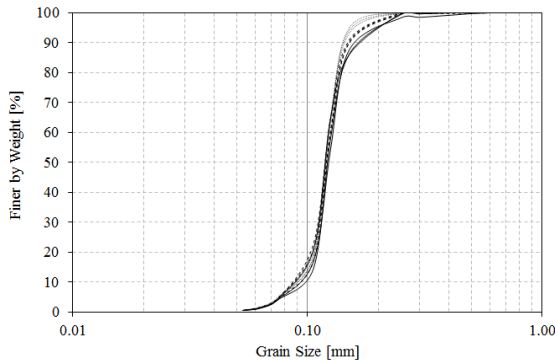

Figure 2. Grain size distribution curves of nine silica sand samples (Maghsoudloo et al. 2018)

4 LARGE SCALE TEST AT 1g

The 1g Liquefaction Tank (De Jager et al 2017), which was used in this experiment, is a 5 m by 2 m by 2 m inclinable container. The tank has two glass side walls. The failure is initiated by tilting the tank to simulate the steepening of submarine slopes due to scouring. A horizontal layer of loose sand sample (with relative density of $Dr \approx$ 30%) with the thickness of 0.5 m is prepared in the 1g Liquefaction Tank using fluidization. Fluidization technique was selected as the most uniform and the most repeatable sample preparation method in this research. The deposited sand in the liquefaction tank was fluidized by a controlled upward flow of water and afterwards allowed to settle down under self-weight of the particles. After stopping the fluidization, the relatively fast consolidation settlements under the self-weight of the sand particles with extremely compressive skeleton occurred. Reproducibility of the experiment results were also verified by repeating each test for three times which resulted in the same values both in terms of density and failure angle. Figure 3 illustrates the early stages of failure recorded by a camera from the transparent longitudinal side of the liquefaction tank.
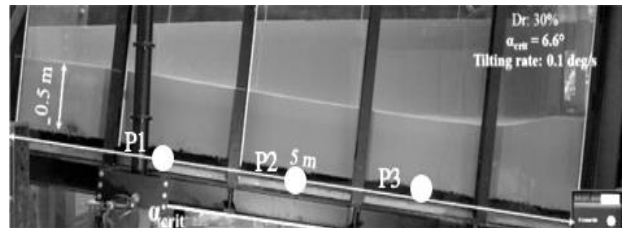

Figure 3. Static liquefaction failure in loose sample with Dr = 30% using the Liquefaction Tank (Maghsoudloo et al. 2017)

Figure 4 shows the pore water pressure differences during the experiment, recorded by three pore pressure transducers (PPT) (P1, P2, and P3) installed on the base centreline of the Liquefaction Tank (locations of PPTs are shown in Figure 3).
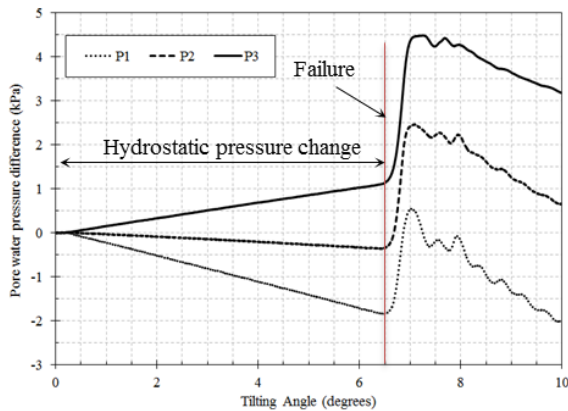
Figure 4. Pore water pressure change during tilting and at the failure of the slope in the 1g Liquefaction Tank

The initial decrease in the hydrostatic pore water pressure measured at P1 and P2 is due to the locations of these sensors with respect to the rotation centre of the tank. The results indicate that static liquefaction failure can be characterized by a sudden jump in the pore water pressures, which occurred at the angle of 6.6 (deg).

5 CENRIFUGE TESTS

A strongbox has been constructed for the beam geo-centrifuge at TU Delft with two transparent side walls. Samples with a length of 355 mm, a width of 134 mm and height of 85 - 87 mm, in model scale, can be tested (Figure 5). The pore pressure developments in the soil layer inside the strongbox can be monitored by three transducers (PPTs, MPXH6400A) during the sample preparation and testing.

A single-plane rotatable set-up was designed to study submarine landslides induced by the steepening of slope angle caused either by the scouring effect or human actives, such as dredging. The set-up can rotate using a linear motor (Linak 282100-40150100, capacity: 1 kN). A potentiometer (S13FLP25A) linking the base plate and the centrifuge basket is used to measure the tilting angle.

Figure 5. Schematic sketch of the newly developed static liquefaction triggering actuator for the geo-centrifuge at TU Delft

The maximum tilting angle is 20º. By controlling the linear motor, the strongbox can rotate with rates ranging from 0.1º/s to 2.0º/s with a precision of 0.002 º/s.

5.1 Pore Fluid

In this study, de-aired viscous fluid was used as the pore fluid and submerging liquid. The viscous fluid was made of Hydroxypropyl Methylcellulose (HPMC) powder. Since centrifuge test was conducted at 10g, the viscosity of the pore fluid was selected to be $\sqrt{N} = 3.3$ times larger than that of water.

5.2 Sample preparation

Fluidization technique has been applied as the sample preparation technique to simulate the formation of a seabed/riverbed in nature and resembles the technique used for the test in the 1g Liquefaction Tank. The fluidization system is integrated to the base of the strongbox.

　　　　　　　　　　　　　　　　4

5.3 Test results

A centrifuge test has been performed on a loose sand layer with a thickness of 50 mm at 10g. The relative density of the sample after preparation at 1g was measured to be 31%. However, due to increase of the g-level and consolidation the relative density increased by approximately 10%. The details of the test are listed in Table 2. The slope showed a sudden failure at 10.5° (Figure 6).

Table 2. Summary of the centrifuge test specifications

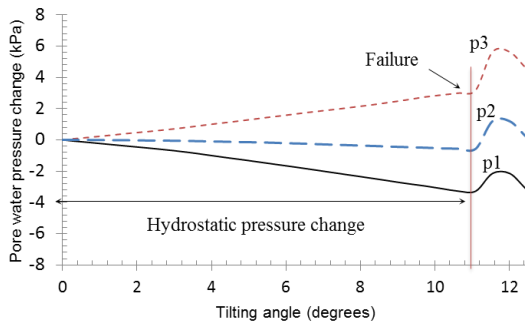| Test Name	Tilting rate (°/s)	$Dr_{\_1g}$	$Dr_{\_10g}$ (%)	Failure angel (°)
Cent	1	31	41	10.5

Figure 6. Changes in pore water pressure for the test in the centrifuge

6 COMPARISON OF RESULTS AND CONCLUSIONS

The evolution of the pore water pressure at the base of both sand layers during the tilting process show similar regime (Figure 4and Figure 6). The first part of the curves shows a hydrostatic linear change in the pore water pressure. Implying a drained monotonic loading on the samples. However, the pore pressures start to increase in a very sudden manner at a certain slope angle. The maximum increment of the pore pressure was measured by the sensor p3, which is located at the lower of the slope during the rotation (refer to Figure 3 and Figure 5). The maximum excess

pore pressure measured by these sensors for both cases of 1g and centrifuge test is ~2.5 kPa. Comparing the values of excess pore pressure and the normal effective stress at this location indicates full liquefaction of the layer.

Despite similarities in the pore pressure regime, the slope angles at failure for both centrifuge test and the 1g-large scale test are different (i.e. 6.6 degrees for the sample in the 1g Liquefaction Tank and 10.5 degrees for the centrifuge sample). The main reason for this difference can be attributed to the difference in the relative densities of the samples prior to tilting (30% for the sample in the liquefaction tank and 41% for the sample in the centrifuge).

7 CONCLUSION

The small scale submerged slopes have been tested in the centrifuge under 10g condition and the results were compared to the large scale 1g test. Viscous fluid with a viscosity of √N-time higher than that of water should be used as the pore and submerging fluid.

The instabilities were triggered by static liquefaction of the slopes using gradual tilting of the slopes to simulate the scouring of the seabed in the vicinity of offshore foundations.

It is concluded that centrifuge technique can be successfully utilised to study the triggering mechanism of submarine statically liquefied submarine landslides.

The combination of generation and dissipation of pore pressure governs the potential of static liquefaction and the scaling law for time.

No measureable precursors could be detected long before the onset of statically liquefied submarine landslide. For the text, a maximum of three levels of sections and subsections is allowed.

8 ACKNOWLEDGEMENTS

9 REFERENCES

Askarinejad A, Beck A, Springman SM (2014) Scaling law of static liquefaction mechanism in geocentrifuge and corresponding hydromechanical characterization of an unsaturated silty sand having a viscous pore fluid. *Canadian Geotechnical Journal* 52(6):708-720. 10.1139/cgj-2014-0237

Askarinejad A, Zhang W, de Boorder M, van der Zon J (2018) Centrifuge and numerical modelling of static liquefaction of fine sandy slopes. In: Physical Modelling in Geotechnics, Volume 2. CRC Press, pp 1119-1124

Byrne P et al. (2000) CANLEX full-scale experiment and modelling. *Canadian geotechnical journal* 37(3):543-562

Chu J, Leroueil S, Leong WK (2003) Unstable behaviour of sand and its implication for slope stability. *Canadian Geotechnical Journal* 40:873-885

Darcy H (1856) Les fontaines publiques de la ville de Dijon. Paris

De Groot M, Lindenberg J, Mastbergen D, Van den Ham G (2012) Large scale sand liquefaction flow slide tests revisited. 1-22. *Proc. Eurofuge*, Delft, The Netherlands.

De Jager RR, Maghsoudloo A, Askarinejad A, Molenkamp F (2017) Preliminary results of instrumented laboratory flow slides. 212-219. *Proceedings of the 1st International Conference on the Material Point Method*

Eckersley JD (1990) Instrumented laboratory flowslides. *Géotechnique* 40:489-502

Kramer S (1988) Triggering of liquefaction flow slides in coastal soil deposits. *Engineering Geology* 26(1):17-31

Lade PV (1992) Static instability and liquefaction of loose fine sandy slopes. *Journal of Geotechnical Engineering* 118(1):51-71

Maghsoudloo A, Askarinejad A, de Jager R, Molenkamp F, Hicks M (2018) Experimental investigation of pore pressure and acceleration development in static liquefaction induced failures in submerged slopes. In: Physical Modelling in Geotechnics, Volume 2. CRC Press, pp 987-992

Maghsoudloo A, Galavi V, Hicks M, Askarinejad A (2017) Finite element simulation of static liquefaction of submerged sand slopes using a multilaminate model. 805-808. *19th International Conference on Soil Mechanics and Geotechnical Engineering*, Seoul.

Masson DG, Harbitz CB, Wynn RB, Pedersen G, Løvholt F (2006) Submarine landslides: processes, triggers and hazard prediction. *Philosophical Transactions of the Royal Society of London A: Mathematical, Physical and Engineering Sciences* 364(1845):2009-2039. 10.1098/rsta.2006.1810

Sladen J, D'hollander R, Krahn J (1985) The liquefaction of sands, a collapse surface approach. *Canadian Geotechnical Journal* 22(4):564-578

Take WA, Bolton MD, Wong PCP, Yeung FJ (2004) Evaluation of landslide triggering mechanisms in model fill slopes. *Landslides* 1:173-184